

Pattern formation in three species food web model in spatiotemporal domain with Beddington–DeAngelis functional response

Randhir Singh Baghel^a, Joydip Dhar^b

^aSchool of Mathematics and Allied Sciences, Jiwaji University
Gwalior-474011, India
randhirsng@gmail.com

^bABV – Indian Institute of Information Technology and Management
Gwalior-474015, India
jdhar@iiitm.ac.in

Received: 23 October 2012 / **Revised:** 4 October 2013 / **Published online:** 19 February 2014

Abstract. A mathematical model is proposed to study a three species food web model of prey-predator system in spatiotemporal domain. In this model, we have included three state variables, namely, one prey and two first order predators population with Beddington-DeAngelis predation functional response. We have obtained the local stability conditions for interior equilibrium and the existence of Hopf-bifurcation with respect to the mutual interference of predator as bifurcation parameter for the temporal system. We mainly focus on spatiotemporal system and provided an analytical and numerical explanation for understanding the diffusion driven instability condition. The different types of spatial patterns with respect to different time steps and diffusion coefficients are obtained. Furthermore, the higher-order stability analysis of the spatiotemporal domain is explored.

Keywords: food web, Hopf-bifurcation, reaction diffusion mechanism, spatial patterns, higher order stability.

1 Introduction

The foundation of population ecology was laid by animal ecologist in the first half of this century. A group of organism of the same species, which survive together in one ecological area at the same time is called a population. Within a population, all the individuals capable of reproduction have the opportunity to reproduce with other mature members of the group. Populations are always changing, hence, they are dynamic in nature [1–5].

The increasing population of the world could attract the attention of not only the ecologist but also of behavioral scientists. It is one of the important issues in ecology to identify some general properties about the structure (for instance, see [6] and its references). The length of food chain is one of the important features interesting for such theoretical studies. This is one of the method to estimate the energy (or a certain material)

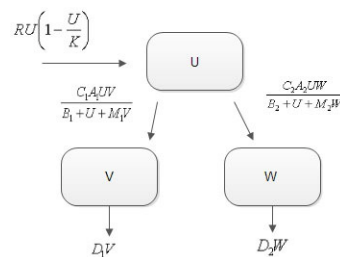


Fig. 1. Schematic diagram of proposed model.

is transferred from a primary producer to a consumer. The average number of links from each producer or each top predator is regarded as the length of food chain [7]. Although the network of energy flows in a food web is in general rather complex, it could be theoretically simplified to a linear chain of energy flows using the method discussed by Murray [8] and Britton [9] and along their theory, we could resolve and reconstruct the network of energy flows into a linear chain for a food web.

Many researchers have used two species model for pattern formation based on coupled reaction diffusion equations. The necessary and sufficient condition for diffusion driven instability, which leads to the formation of spatial patterns, has been derived and very interesting patterns have also been observed from the numerical simulations [10–14].

Recently researchers have studied the formation of patterns for different three species interacting discrete or continuous systems [1, 5, 15–17]. Most of the authors have considered a food chain model with diffusion and investigated the diffusion driven instability in the spatial system.

Keeping in view the above discussion, we will study a food web model for one prey and two predator system with Beddington–DeAngelis functional response (see Fig. 1).

The main contribution in this paper is to study the effect of diffusion on the three species food web model with Beddington–DeAngelis functional response. We have obtained analytically as well numerically the diffusion driven instability condition for the spatial system. In addition, we have obtained the different types of spatial patterns. Finally, the higher order stability analysis for the three species prey-predator system has explored.

The rest of this paper is organized as follows. In Section 2, we have proposed spatiotemporal mathematical model, Section 3 presents the local stability analysis and Hopf-bifurcation for the temporal system. In Section 4, we have derived the analytical conditions for diffusion driven instability and the numerical simulation are performed. In Section 5, the higher order stability analysis is discussed. Finally, conclusion is given in last Section 6.

2 The mathematical model

A mathematical model of one prey utilized by two predators has been studied in temporal domain with Beddington–DeAngelis functional response [2]. Motivated from the work

and to make more realistic one, we extend this model in spatiotemporal domain to study it's spatial dynamics. Let U , V and W are the population densities of prey and two predators, respectively, at time T and spatial location (X, Y) . Similar as in [2], the trophic function between prey species and predator species has been described by a Beddington–DeAngelis functional response with a maximum grazing rate A_i and fixed half saturation value B_i , $i = 1, 2$, for two predators. The factors M_i denotes mutual interference of predators of the same species. The parameter C_i represents the conversion ratios of prey to respective predators. Moreover, the prey species grow logistically with a intrinsic growth rate R and carrying capacity K . The factors D_i , $i = 1, 2$, are the death rates of predators species V and W , respectively. Finally, \widehat{D}_a , \widehat{D}_b and \widehat{D}_c are diffusivity coefficients for prey and predators population, respectively. Thus the mathematical model governing the spatiotemporal dynamics of the three interacting species in the prey-predator community can be described by the following system of reaction-diffusion equations:

$$\frac{\partial U}{\partial T} = RU \left(1 - \frac{U}{K} \right) - \frac{A_1 UV}{B_1 + U + M_1 V} - \frac{A_2 UW}{B_2 + U + M_2 W} + \widehat{D}_a \nabla^2 U, \quad (1)$$

$$\frac{\partial V}{\partial T} = \frac{C_1 A_1 UV}{B_1 + U + M_1 V} - D_1 V + \widehat{D}_b \nabla^2 V, \quad (2)$$

$$\frac{\partial W}{\partial T} = \frac{C_2 A_2 UW}{B_2 + U + M_2 W} - D_2 W + \widehat{D}_c \nabla^2 W \quad (3)$$

with non-negative initial conditions $U(0), V(0), W(0) \geq 0$. It is assumed that all parameters are positive constants. The subject to the no-flux boundary conditions and known positive initial distribution of populations are described by

$$U(X, Y, 0) > 0, \quad V(X, Y, 0) > 0, \quad W(X, Y, 0) > 0, \quad (X, Y) \in \Omega, \quad (4)$$

$$\frac{\partial U}{\partial n} = \frac{\partial V}{\partial n} = \frac{\partial W}{\partial n} = 0, \quad (X, Y) \in \partial\Omega, \quad T > 0. \quad (5)$$

Here $\nabla^2 = \partial^2/\partial X^2 + \partial^2/\partial Y^2$ is the Laplacian operator in two-dimensional cartesian coordinate system, Ω is 2D bounded rectangular domain with boundary $\partial\Omega$, $\partial/\partial n$ is the outward drawn normal derivative on the boundary, $\widehat{D}_a, \widehat{D}_b, \widehat{D}_c$ are positive constant diffusion coefficients for one prey and two predators population respectively.

To reduce the number of parameters of the system (1)–(3), we use the following transformations:

$$t = RT, \quad u = \frac{U}{K}, \quad v = \frac{A_1 V}{RK}, \quad w = \frac{A_2 W}{RK},$$

$$x = \frac{X}{\lambda}, \quad y = \frac{Y}{\lambda}, \quad \lambda = \sqrt{\frac{1}{R}}.$$

After, these substitutions we get the following system of equations (for more details, see [2]), where u, v, w are new scaled measures of population size; D_a, D_b, D_c are

non-dimensionalized the diffusion coefficients and t is a new variable of time:

$$\frac{\partial u}{\partial t} = u(1-u) - \frac{uv}{b_1 + u + m_1v} - \frac{uw}{b_2 + u + m_2w} + D_a \nabla^2 u, \quad (6)$$

$$\frac{\partial v}{\partial t} = \frac{a_1 uv}{b_1 + u + m_1v} - d_1 v + D_b \nabla^2 v, \quad (7)$$

$$\frac{\partial w}{\partial t} = \frac{a_2 uw}{b_2 + u + m_2w} - d_2 w + D_c \nabla^2 w. \quad (8)$$

The positive initial distributions and no-flux boundary conditions become

$$u(x, y, 0) > 0, \quad v(x, y, 0) > 0, \quad w(x, y, 0) > 0, \quad (x, y) \in \Omega, \quad (9)$$

$$\frac{\partial u}{\partial n} = \frac{\partial v}{\partial n} = \frac{\partial w}{\partial n} = 0, \quad (x, y) \in \partial\Omega, \quad t > 0. \quad (10)$$

In equations (6)–(8), $a_1, a_2, b_1, b_2, m_1, m_2, d_1, d_2$ are positive constant coefficients. Here u, v and w stand for the population densities of one prey and two predators at any instant of time t and at any point $(x, y) \in \Omega$. Also the no-flux boundary conditions are used.

In the next section, we will study the dynamics of the corresponding temporal system of the spatiotemporal system (6)–(8).

3 Analysis of temporal system

In this section, we will study the dynamical behavior of system (6)–(8) in the absence of diffusion, (i.e., taking diffusion coefficients D_a, D_b and D_c equal to zero) and populations are homogeneous through out the space. Hence, the corresponding temporal system is given by

$$\frac{du}{dt} = u(1-u) - \frac{uv}{b_1 + u + m_1v} - \frac{uw}{b_2 + u + m_2w}, \quad (11)$$

$$\frac{dv}{dt} = \frac{a_1 uv}{b_1 + u + m_1v} - d_1 v, \quad (12)$$

$$\frac{dw}{dt} = \frac{a_2 uw}{b_2 + u + m_2w} - d_2 w. \quad (13)$$

Here all the parameters are strictly positive constants. There are five biologically feasible steady states: $E_0 = (0, 0, 0)$, $E_1 = (1, 0, 0)$, $E_2 = (\hat{u}, \hat{v}, 0)$, $E_3 = (\tilde{u}, 0, \tilde{w})$ and $E^* = (u^*, v^*, w^*)$ for system (11)–(13) (for more details about the steady states and stability of system, see [2]). Here we mainly focus on interior equilibrium $E^* = (u^*, v^*, w^*)$, where $v^* = (u^*(a_1 - d_1) - b_1 d_1)/(d_1 m_1)$, $w^* = (u^*(a_2 - d_2) - b_2 d_2)/(d_2 m_2)$ and the unique positive u^* is given by

$$u^{*2} + \left(\frac{a_1 - d_1}{a_1 m_1} + \frac{a_2 - d_2}{a_2 m_2} - 1 \right) u^* - \left(\frac{b_1 d_1}{a_1 m_1} + \frac{b_2 d_2}{a_2 m_2} \right) = 0.$$

Hence, the interior equilibrium E^* exists only when $u^*(a_1 - d_1) > b_1 d_1$ and $u^*(a_2 - d_2) > b_2 d_2$ holds. The general variation matrix corresponding to system (11)–(13) is given by

$$J^* = \begin{bmatrix} a_{11} & a_{12} & a_{13} \\ a_{21} & a_{22} & a_{23} \\ a_{31} & a_{32} & a_{33} \end{bmatrix},$$

where

$$\begin{aligned} a_{11} &= 1 - \frac{v}{b_1 + u + m_1 v} - \frac{w}{b_2 + u + m_2 w} \\ &\quad + u \left(-2 + \frac{v}{(b_1 + u + m_1 v)^2} + \frac{w}{(b_2 + u + m_2 w)^2} \right), \\ a_{12} &= -\frac{u(b_1 + u)}{(b_1 + u + m_1 v)^2}, \quad a_{13} = -\frac{u(b_2 + u)}{(b_2 + u + m_2 w)^2}, \\ a_{21} &= \frac{a_1 v(b_1 + m_1 v)}{(b_1 + u + m_1 v)^2}, \quad a_{22} = -d_1 + \frac{a_1 u(b_1 + u)}{(b_1 + u + m_1 v)^2}, \quad a_{23} = 0, \\ a_{31} &= \frac{a_2 w(b_2 + m_2 w)}{(b_2 + u + m_2 w)^2}, \quad a_{32} = 0, \quad a_{33} = -d_2 + \frac{a_2 u(b_2 + u)}{(b_2 + u + m_2 w)^2}. \end{aligned}$$

The characteristic equation for the equilibrium $E^* = (u^*, v^*, w^*)$ is

$$\lambda^3 + A_1 \lambda^2 + A_2 \lambda + A_3 = 0. \tag{14}$$

The constant coefficients A_1 , A_2 and A_3 can be easily calculate from the above general variation matrix. From Routh–Hurwitz criteria it follows that E^* is locally stable if $A_i > 0$, $i = 1, 2, 3$, and $A_1 A_2 > A_3$.

3.1 Existence of Hopf-bifurcation

Now, we will study the Hopf-bifurcation of above system, taking m_1 (i.e., mutual interference of predators) as the bifurcation parameter. Again, the necessary and sufficient conditions for the existence of the Hopf-bifurcation if there exists $m_1 = m_{10}$ such that:

- (i) $A_i(m_{10}) > 0$, $i = 1, 2, 3$,
- (ii) $A_1(m_{10})A_2(m_{10}) - A_3(m_{10}) = 0$ and
- (iii) $\text{Re}(du_i/dr) \neq 0$, $i = 1, 2, 3$, where u_i is the real parts of the eigenvalues of the characteristic equation (14) of the form $\lambda_i = u_i + iv_i$.

Now, we will verify the condition (iii) of Hopf-bifurcation. Put $\lambda = u + iv$ in (14), we get

$$(u + iv)^3 + A_1(u + iv)^2 + A_2(u + iv) + A_3 = 0. \tag{15}$$

On separating the real and imaginary parts and eliminating v between real and imaginary parts, we get

$$8u^3 + 8A_1u^2 + 2(A_1^2 + A_2)u + A_1A_2 - A_3 = 0. \tag{16}$$

Now, we have $u(m_{10}) = 0$ as $A_1(m_{10})A_2(m_{10}) - A_3(m_{10}) = 0$. Further, $m_1 = m_{10}$, is the only positive root of $A_1(m_{10})A_2(m_{10}) - A_3(m_{10}) = 0$, and the discriminant of

$8u^2 + 8A_1u + 2(A_1^2 + A_2) = 0$ is $-64A_2 < 0$. Here differentiating (16) with respect to m_1 , then we get

$$\begin{aligned} & (24u^2 + 16A_1u + 2(A_1^2 + A_2)) \frac{du}{dm_1} + (8u^2 + 4A_1u) \frac{dA_1}{dm_1} \\ & + 2u \frac{dA_2}{dm_1} + \frac{d}{dm_1}(A_1A_2 - A_3) = 0. \end{aligned}$$

Now, since at $m_1 = m_{10}$, $u(m_{10}) = 0$, we obtain

$$\left[\frac{du}{dm_1} \right]_{m_1=m_{10}} = \frac{-\frac{d}{dm_1}(A_1A_2 - A_3)}{2(A_1^2 + A_2)} \neq 0.$$

The parametric values are $a_1 = 0.3$, $a_2 = 0.2$, $d_1 = 0.03$, $d_2 = 0.02$, $b_1 = 0.5$, $m_2 = 0.5$, $b_2 = 0.6$, which ensures that the above system has a Hopf-bifurcation. It is shown graphically in Fig. 2.

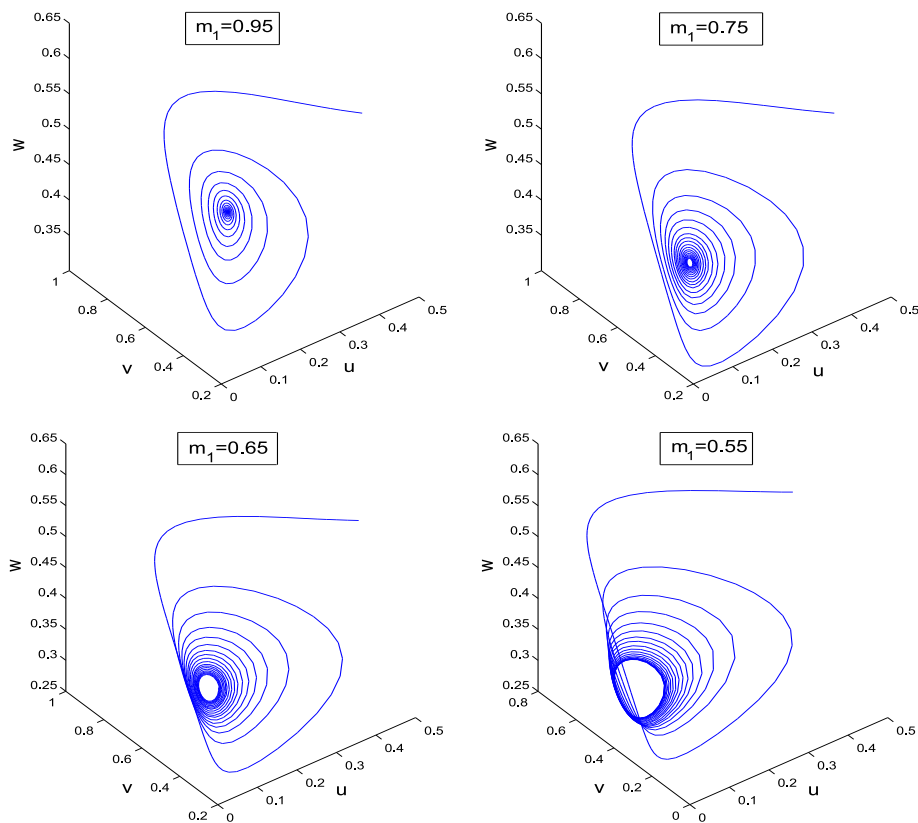


Fig. 2. The phase representation of three species around the interior equilibrium.

4 Analysis of the spatiotemporal model

Now, we will study the effect of diffusion in the most interesting spatially homogenous interior equilibrium E^* , $v^* = (u^*(a_1 - d_1) - b_1d_1)/(d_1m_1) > 0$, and $w^* = (u^*(a_2 - d_2) - b_2d_2)/(d_2m_2) > 0$ of the reaction diffusion system (6)–(8). Obviously, the interior equilibrium point E^* for the non-spatial system is a spatially homogeneous steady-state for the reaction-diffusion system (6)–(8). We assume that E^* is the non-spatially homogeneous equilibrium is stable with respect to spatially homogeneous following perturbation:

$$u(x, y, t) = u^* + \epsilon \exp((kx + ky)i + \lambda_k t), \tag{17}$$

$$v(x, y, t) = v^* + \eta \exp((kx + ky)i + \lambda_k t), \tag{18}$$

$$w(x, y, t) = w^* + \rho \exp((kx + ky)i + \lambda_k t), \tag{19}$$

where ϵ, η and ρ are chosen to be small and $k^2 = (k_x^2 + k_y^2)$ is the wave number. Substituting (17)–(19) into (6)–(8), linearizing the system around the interior equilibrium E^* , we get the characteristic equation as follows:

$$|J_k - \lambda_k I_2| = 0 \tag{20}$$

with

$$J_k = \begin{bmatrix} a_{11} - D_a k^2 & a_{12} & a_{13} \\ a_{21} & a_{22} - D_b k^2 & a_{23} \\ a_{31} & a_{32} & a_{33} - D_c k^2 \end{bmatrix}.$$

The eigenvalues are the solutions of the characteristic equation

$$\lambda^3 + p_2(k^2)\lambda^2 + p_1(k^2)\lambda + p_0(k^2) = 0. \tag{21}$$

The coefficients p_2, p_1 and p_0 can be found from the above matrix J_k .

According to the Routh–Hurwitz criterion, all the eigenvalues have negative real parts if and only if the following conditions hold:

$$p_2(k^2) > 0, \tag{22}$$

$$p_0(k^2) > 0, \tag{23}$$

$$Q = p_0(k^2) - p_1(k^2)p_2(k^2) < 0. \tag{24}$$

This is best understood in terms of the invariants of the matrix and of its inverse matrix

$$J_k^{-1} = \frac{1}{\det(J_k)} \begin{pmatrix} M_{11} & M_{12} & M_{13} \\ M_{21} & M_{22} & M_{23} \\ M_{31} & M_{32} & M_{33} \end{pmatrix},$$

where

$$M_{11} = \frac{a_1 a_2 m_1 m_2 u^2 v w}{(b_1 + u + m_1 v)^2 (b_2 + u + m_2 w)^2},$$

$$M_{12} = -\frac{(b_1 + u) a_2 m_2 u^2 w}{(b_1 + u + m_1 v)^2 (b_2 + u + m_2 w)^2},$$

$$\begin{aligned}
M_{13} &= -\frac{(b_2 + u)a_1 m_1 u v w}{(b_1 + u + m_1 v)^2 (b_2 + u + m_2 w)^2}, \\
M_{21} &= \frac{(b_1 + m_1 v)a_1 a_2 m_2 u v w}{(b_2 + u + m_2 w)^2}, \\
M_{22} &= -\frac{a_2 m_2 u w}{(b_2 + u + m_2 w)^2} \left(1 - 2u - \frac{(b_1 + m_1 v)v}{(b_1 + u + m_1 v)^2} - \frac{(b_2 + m_2 w)w}{(b_2 + u + m_2 w)^2} \right) \\
&\quad + \frac{(b_2 + u)(b_2 + m_2 w)a_2 w^2}{(b_2 + u + m_2 w)^4}, \\
M_{23} &= -\frac{(b_2 + u)(b_1 + m_1 v)a_1 v w}{(b_1 + u + m_1 v)^2 (b_2 + u + m_2 w)^2}, \\
M_{31} &= \frac{a_1 a_2 m_1 u v w}{(b_1 + u + m_1 v)^2 (b_2 + u + m_2 w)^2}, \\
M_{32} &= -\frac{(b_2 + m_2 u)(b_1 + u)a_2 u w}{(b_1 + u + m_1 v)^2 (b_2 + u + m_2 w)^2}, \\
M_{33} &= -\frac{a_1 m_1 u v}{(b_1 + u + m_1 v)^2} \left(1 - 2u - \frac{(b_1 + m_1 v)v}{(b_1 + u + m_1 v)^2} - \frac{(b_2 + m_2 w)w}{(b_2 + u + m_2 w)^2} \right) \\
&\quad + \frac{(b_1 + u)(b_1 + m_1 v)a_1 u v}{(b_1 + u + m_1 v)^4}.
\end{aligned}$$

Here matrix M_{ij} is the adjunct of J_k .

We obtain the following conditions of the steady-state stability (i.e., stability for any value of k): (i) all diagonal cofactors of matrix J_k must be positive; (ii) all diagonal elements of matrix J_k must be negative. The two above condition taken together are sufficient to ensure stability of a give steady state. It means that instability for some $k > 0$ can only be observed if at least one of them is violated. Thus we arrive at the following necessary condition for the Turing instability [15, 18]: (i) the largest diagonal element of matrix J_k must be positive and/or (ii) the smallest diagonal cofactor of matrix J_k must be negative. By the Routh–Hurwitz criteria, instability takes place if and only if one of the conditions (22)–(24) is broken. We consider (23) for instability condition

$$\begin{aligned}
p_0(k^2) &= D_a D_b D_c k^6 - (D_a D_b a_{33} + D_b D_c a_{11} + D_a D_c a_{22}) k^4 \\
&\quad + (D_a M_{11} + D_b M_{22} + D_c M_{33}) k^2 - \det J_k.
\end{aligned} \tag{25}$$

According to Routh–Hurwitz criterion, $p_0(k^2) < 0$ is sufficient condition for matrix J_k being unstable. Let us assume that $M_{33} < 0$. If we choose $D_a = 0$, $D_b = 0$, then

$$\begin{aligned}
p_0(k^2) &= D_c M_{33} k^2 - \det(J_k) \\
&= \frac{1}{(b_1 + u + m_1 v)^2 (b_2 + u + m_2 w)^2} (a_1 u (b_1 + u) ((b_2 + u)(-1 + 2u) \\
&\quad \times (-a_2 u + (d_2 + D_c k^2)(b_2 + u))) + (d_2 + D_c k^2)(2m_2 u(-1 + 2u) \\
&\quad + b_2(1 + m_2(-2 + 4u)))w + (d_2 + D_c k^2)m_2(1 + m_2(-1 + 2u))w^2)
\end{aligned}$$

$$\begin{aligned}
 & - \frac{1}{m_2(b_1 + u + m_1v)^2} ((d_2 + D_c k^2) ((b_1 + u)^2 (1 + m_2(-1 + 2u)) \\
 & + (2m_1u(1 + m_2(-1 + 2u)) + b_1(m_2 + m_1(2 - 2m_2 + 4m_2u)))v \\
 & + m_1(m_1 + m_2 - m_1m_2 + 2m_1m_2u)v^2)) \\
 & + \frac{u(b_2 + u)}{(b_1 + u + m_1v)^2(b_2 + u + m_2w)^2} \\
 & \times \left((d_2 + D_c k^2 + a_2m_2(1 - 2u))(b_1 + u)^2 \right. \\
 & + (2m_1u(d_2 + D_c k^2 + a_2m_2 - 2a_2m_2u) \\
 & + b_1(-a_2m_2 + 2m_1(d_2 + D_c k^2 + a_2m_2 - 2a_2m_2u)))vm_1 \\
 & \left. \times (d_2m_1 + D_c k^2m_1 + a_2m_2(-1 + m_1 - 2m_1u)v^2) - \frac{(d_2 + D_c k^2)(b_2 + 2u)}{b_2 + u + m_2w} \right) \\
 & + \frac{1}{(b_1 + u + m_1v)^4} \left(a_1D_c k^2uv(b_1 + u)v(b_1 + m_1v) - m_1(b_1 + u + m_1v)^2 \right. \\
 & \left. \times \left(1 - 2u - \frac{v(b_1 + m_1v)}{(b_1 + u + m_1v)^2} - \frac{w(b_2 + m_2w)}{(b_2 + u + m_2w)^2} \right) \right) < 0 \quad \forall k > k_c, \quad (26)
 \end{aligned}$$

where $k_c > 0$ is the small critical wave number. Hence, in this system, diffusion-driven instability occurs, i.e., the small spatio-temporal perturbations around the homogeneous steady-state are unstable and, hence, of generation of spatio-temporal pattern is justified.

Now, we obtained the eigenvalues of the characteristic equation (21) numerically of the spatial system (6)–(8). Here we choose some parametric values of $a_1 = 0.3$, $a_2 = 0.2$, $d_1 = 0.03$, $d_2 = 0.02$, $b_1 = 0.5$, $b_2 = 0.6$, $m_2 = 0.5$, $m_1 = 0.4$, $D_a = 0.0$, $D_b = 0.0$, $D_c = 0.3$, in this set of values, $p_0(k^2) < 0$ for all $k > 0.01$, hence, from (26), we can observe diffusion driven instability of the system. For same set of parametric values with different diffusion rates, the real part of largest eigenvalue are calculated and illustrated in Fig. 3: (a) $D_a = 0.3$, $D_b = 0.2$, $D_c = 0.1$; (b) $D_a = 0.4, 0.7, 1.0$, $D_b = 0.2$, $D_c = 0.1$; (c) $D_a = 0.3$, $D_b = 0.1, 0.5, 0.9$, $D_c = 0.1$ and (d) $D_a = 0.3$, $D_b = 0.2$, $D_c = 0.3, 0.6, 1.5$.

4.1 Spatiotemporal pattern formation

It is well known that the analytical solution of the coupled reaction diffusion system is not always possible. Hence, one has to use numerical simulations to solve them. The spatiotemporal system (6)–(8) is solved numerically in two-dimensional space using a finite difference method for the spatial derivatives. In order to avoid numerical artifacts, the values of the time and space steps have been chosen sufficiently small. For the numerical simulations, the initial distributions of the species are considered as small spatial perturbation of the uniform equilibrium. All the numerical simulations use the zero-flux boundary condition in a square habitat of size 200×200 and 100×100 . The iterations are performed for different step sizes in time.

The spatial distributions of prey-predator system in the time evaluation are given in Figs. 4–7. By varying coupling parameters, we observed that if one parameter value

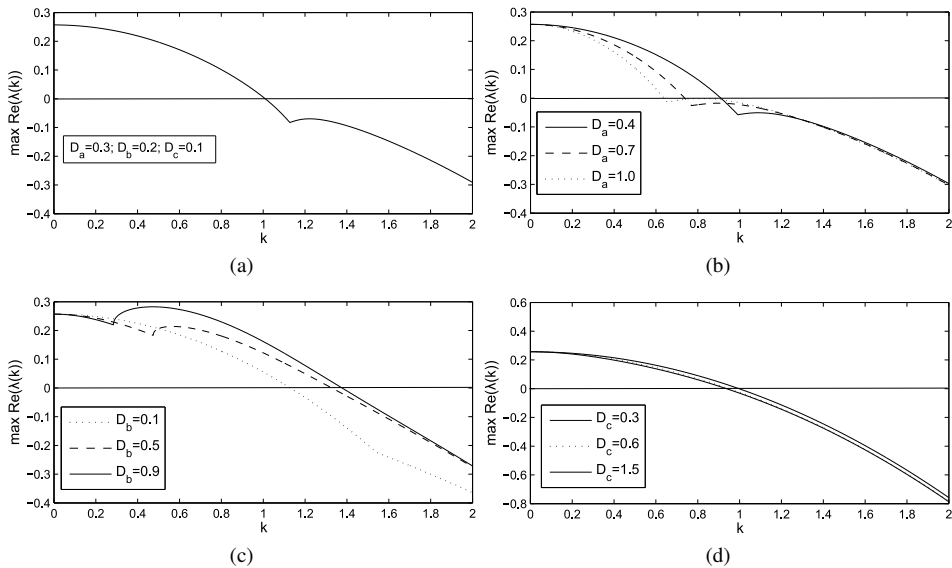


Fig. 3. Plot of $\max \operatorname{Re}(\lambda(k))$ against k . The other parametric values are given in text.

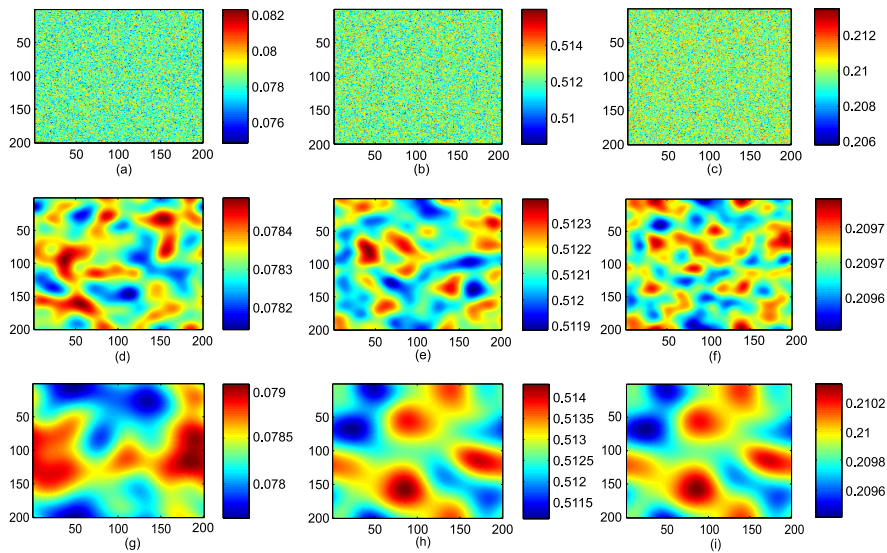


Fig. 4. Spatial distribution of prey (first column), first predator (second column) and second predator (third column) are population densities of the spatial system (6)–(8). Spatial patterns are obtained with diffusivity coefficients $D_a = 0.03$, $D_b = 0.02$, $D_c = 0.01$ at different time levels: for $T = 0$ (a)–(c), $T = 200$ (d)–(f), $T = 1000$ (g)–(i).

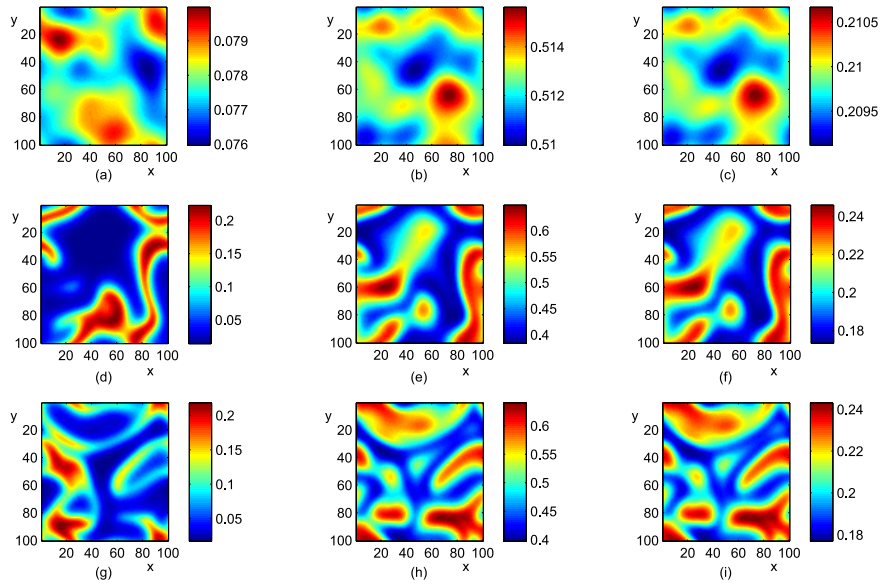


Fig. 5. Spatial distribution of prey (first column), first predator (second column) and second predator (third column) are population densities of the spatial system (6)–(8). Spatial patterns are obtained with diffusivity coefficients $D_a = 0.03$, $D_b = 0.02$, $D_c = 0.01$ at different time levels: for $T = 1000$ (a)–(c), $T = 3000$ (d)–(f), $T = 5000$ (g)–(i).

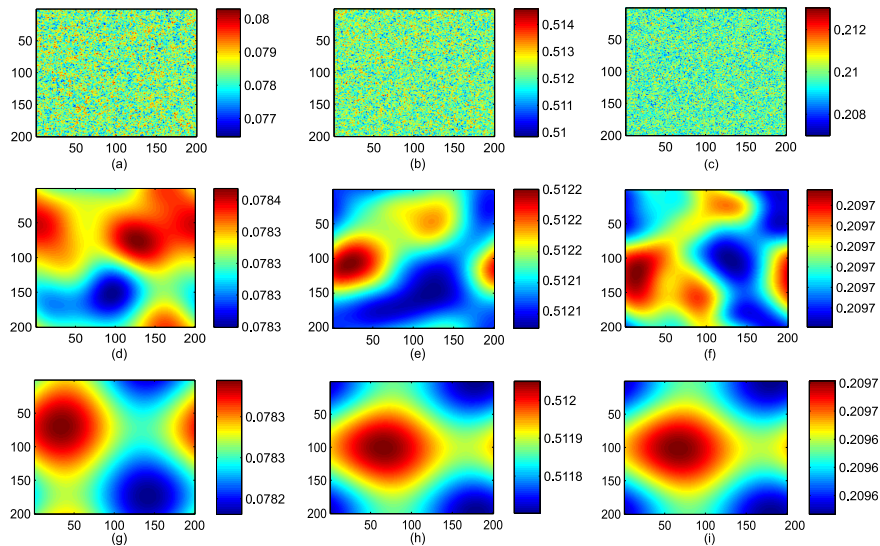


Fig. 6. Spatial distribution of prey (first column), first predator (second column) and second predator (third column) are population densities of the spatial system (6)–(8). Spatial patterns are obtained with diffusivity coefficients $D_a = 0.3$, $D_b = 0.2$, $D_c = 0.1$ at different time levels: for $T = 0$ (a)–(c), $T = 200$ (d)–(f), $T = 1000$ (g)–(i).

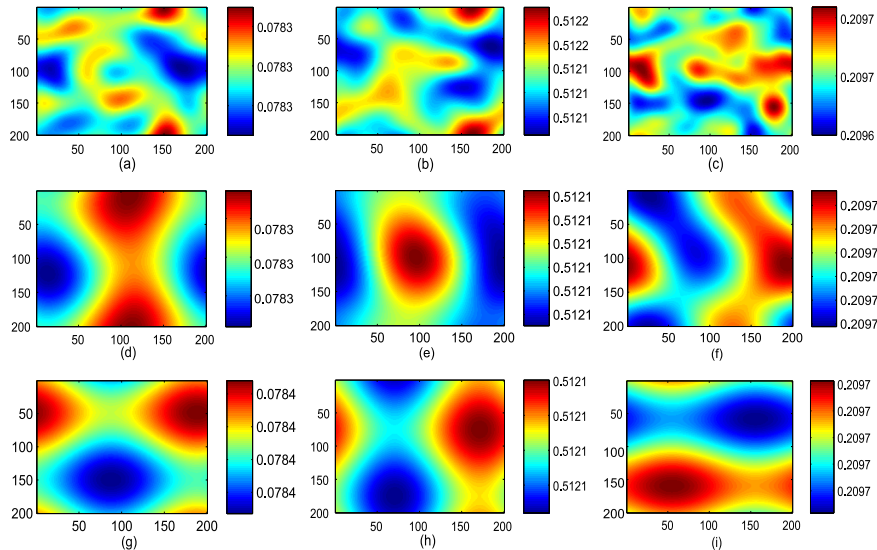


Fig. 7. Spatial distribution of prey (first column), first predator (second column) and second predator (third column) are population densities of the spatial system (6)–(8). Spatial patterns are obtained with diffusivity coefficients $D_a = 3$, $D_b = 2$, $D_c = 1$ at different time levels: for $T = 10$ (a)–(c), $T = 100$ (d)–(f), $T = 500$ (g)–(i).

changes, then spatial structure changes over the times of the spatial system. In Figs. 4–7, we observed well organized structures for the spatial distribution of populations, and also when time T increase, the densities of different classes of population become uniform throughout the space. The parametric values are used same as in Fig. 3.

In Figs. 4 and 6, we have shown the pattern formation with different time steps. It can be observed that a stationary “mixtures \rightarrow stripe-spot mixtures \rightarrow spots” patterns are time-dependent, as similar in [19]. From Figs. 5 and 7, we observed that the pattern sequence are mixtures of “spots \rightarrow stripe” and “spots-stripe \rightarrow spots”, respectively, as in [20–23]. Finally, From Fig. 7, it is observed that the higher diffusivity coefficients stabilized the spatial system.

5 Higher order stability analysis

In this subsection, we will determine the instability conditions by the higher-order spatiotemporal perturbation terms [24]. We choose a general two non-dimensional reaction-diffusion system. System (6)–(8) is recalled with specific choice of parameter values. The three dimensional reaction diffusion systems are described as follows:

$$u_t = f(u, v, w) + D_a(u_{xx} + u_{yy}), \quad (27)$$

$$v_t = g(u, v, w) + D_b(v_{xx} + v_{yy}), \quad (28)$$

$$w_t = h(u, v, w) + D_c(w_{xx} + w_{yy}) \quad (29)$$

with no-flux boundary conditions and initial distribution of population within 2D bounded domain. The interior equilibrium point E^* for the non-spatial system corresponding to the system is a spatially homogeneous equilibrium for system (27)–(29). We consider E^* is locally asymptotically stable equilibrium for the temporal model. Taking the spatial perturbations $u(t, x, y)$, $v(t, x, y)$ and $w(t, x, y)$ on the steady states u^*, v^*, w^* defined by $u = u^* + n(t, x, y)$, $v = v^* + p(t, x, y)$, $w = w^* + m(t, x, y)$ and then expanding the temporal part in Taylor series up to second order around the steady state, we find following three expressions:

$$n_t = f_u n + f_v p + f_w m + \frac{f_{uu}}{2} n^2 + \frac{f_{vv}}{2} p^2 + \frac{f_{ww}}{2} m^2 + f_{uv} np + f_{vw} pm + f_{uw} nm + D_a(n_{xx} + n_{yy}), \tag{30}$$

$$p_t = g_u n + g_v p + g_w m + \frac{g_{uu}}{2} n^2 + \frac{g_{vv}}{2} p^2 + \frac{g_{ww}}{2} m^2 + g_{uv} np + g_{vw} pm + g_{uw} nm + D_b(p_{xx} + p_{yy}), \tag{31}$$

$$m_t = h_u n + h_v p + h_w m + \frac{h_{uu}}{2} n^2 + \frac{h_{vv}}{2} p^2 + \frac{h_{ww}}{2} m^2 + h_{uv} np + h_{vw} pm + h_{uw} nm + D_c(m_{xx} + m_{yy}). \tag{32}$$

Now, taking spatial perturbation in the form of

$$\begin{aligned} n(t, x, y) &= n(t) \cos(k_x x) \cos(k_y y), \\ p(t, x, y) &= p(t) \cos(k_x x) \cos(k_y y), \\ m(t, x, y) &= m(t) \cos(k_x x) \cos(k_y y) \end{aligned}$$

with no-flux boundary condition leads to the following three system of equations:

$$n_t = f_u n + f_v p + f_w m + \frac{f_{uu}}{2} n^2 + \frac{f_{vv}}{2} p^2 + \frac{f_{ww}}{2} m^2 + f_{uv} np + f_{vw} pm + f_{uw} nm - D_a k^2 n, \tag{33}$$

$$p_t = g_u n + g_v p + g_w m + \frac{g_{uu}}{2} n^2 + \frac{g_{vv}}{2} p^2 + \frac{g_{ww}}{2} m^2 + g_{uv} np + g_{vw} pm + g_{uw} nm - D_b k^2 p, \tag{34}$$

$$m_t = h_u n + h_v p + h_w m + \frac{h_{uu}}{2} n^2 + \frac{h_{vv}}{2} p^2 + \frac{h_{ww}}{2} m^2 + h_{uv} np + h_{vw} pm + h_{uw} nm - D_c k^2 m. \tag{35}$$

It is clear from above three equations that the growth or decay of first-order perturbation terms depends upon the second-order perturbation terms. Further, we need the dynamical equations for second-order perturbation terms involved in (33)–(35). Multiplying each term of equation (33) by $2u$ and neglecting the contribution of third-order perturbation terms, we find the dynamical equation for u^2 as

$$(n^2)_t = 2f_u n^2 + 2f_v np + 2f_w nm - 2D_a k^2 n^2, \tag{36}$$

and proceeding in a similar fashion, the dynamical equations for remaining second-order perturbations are given by

$$(p^2)_t = 2g_u np + 2g_v p^2 + 2g_w pm - 2D_b k^2 p^2, \quad (37)$$

$$(m^2)_t = 2h_u nm + 2h_v pm + 2h_w m^2 - 2D_c k^2 m^2, \quad (38)$$

$$(np)_t = g_u n^2 + f_v p^2 + (f_u + g_v) np - k^2(D_a + D_b) np, \quad (39)$$

$$(pm)_t = h_v p^2 + g_w m^2 + g_u nm + h_u np + (g_v + h_w) pm - k^2(D_b + D_c) pm, \quad (40)$$

$$(nm)_t = h_u n^2 + f_w m^2 + f_v pm + h_v np + (f_u + h_w) nm - k^2(D_a + D_c) nm. \quad (41)$$

The truncation of third and higher-order terms in Taylor series expansion and neglecting of third and higher-order perturbation terms during derivation of dynamical equations (33)–(41) leads us to a closed system of equations for $n, p, m, n^2, p^2, m^2, np, pm, nm$. Otherwise, one cannot avoid infinite hierarchy of dynamical equations for perturbation terms. Truncation of higher-order terms does not affect the understanding of the role of leading-order non-linearity. Applicability and significance of the analysis can be justified with the perturbation terms up to order three for system (6)–(8) with suitable choice of parameter values. Consideration of third- and higher-order perturbation terms may be required for this type of analysis use in other system. It also depends upon the non-linearity involved. The dynamical equations (33)–(41) can be written into a compact matrix form as follows:

$$\frac{dX}{dt} = AX, \quad (42)$$

where $X = [n, p, m, n^2, p^2, m^2, np, pm, nm]^T$ and

$$A = \begin{bmatrix} a_{11} & f_v & f_w & f_{uu}/2 & f_{vv}/2 & f_{ww}/2 & f_{uv} & f_{vw} & f_{uw} \\ g_u & a_{22} & g_w & g_{uu}/2 & g_{vv}/2 & g_{ww}/2 & g_{uv} & g_{vw} & g_{uw} \\ h_u & h_v & a_{33} & h_{uu}/2 & h_{vv}/2 & h_{ww}/2 & h_{uv} & h_{vw} & h_{uw} \\ 0 & 0 & 0 & a_{44} & 0 & 0 & 2f_v & 0 & 2f_w \\ 0 & 0 & 0 & 0 & a_{55} & 0 & 2g_u & 2g_w & 0 \\ 0 & 0 & 0 & 0 & 0 & a_{66} & 0 & 2h_v & 2h_u \\ 0 & 0 & 0 & g_u & f_v & 0 & a_{77} & 0 & 0 \\ 0 & 0 & 0 & 0 & h_v & g_w & h_u & a_{88} & g_u \\ 0 & 0 & 0 & h_u & 0 & f_w & h_v & f_v & a_{99} \end{bmatrix}$$

with $a_{11} = f_u - D_a k^2$, $a_{22} = g_v - D_b k^2$, $a_{33} = h_w - D_c k^2$, $a_{44} = 2(f_u - D_a k^2)$, $a_{55} = 2(g_v - D_b k^2)$, $a_{66} = 2(h_w - D_c k^2)$, $a_{77} = f_u + g_v - k^2(D_a + D_b)$, $a_{88} = g_v + h_w - k^2(D_b + D_c)$, $a_{99} = f_u + h_w - k^2(D_a + D_c)$.

Taking solution of system (42) in the form $X(t) \sim e^{\lambda t}$, one can obtain the characteristic equation for the matrix A

$$|A - \lambda I_9| = 0, \quad (43)$$

where $\lambda \equiv \lambda(k)$ are the eigenvalues of A . Thus, required instability condition demands at least one of the eigenvalues of matrix A must have positive real part, i.e., $\text{Re}(\lambda(k)) > 0$ for at least one $r \in (1, 2, 3, \dots, 9)$. Existence of at least one eigenvalue having positive

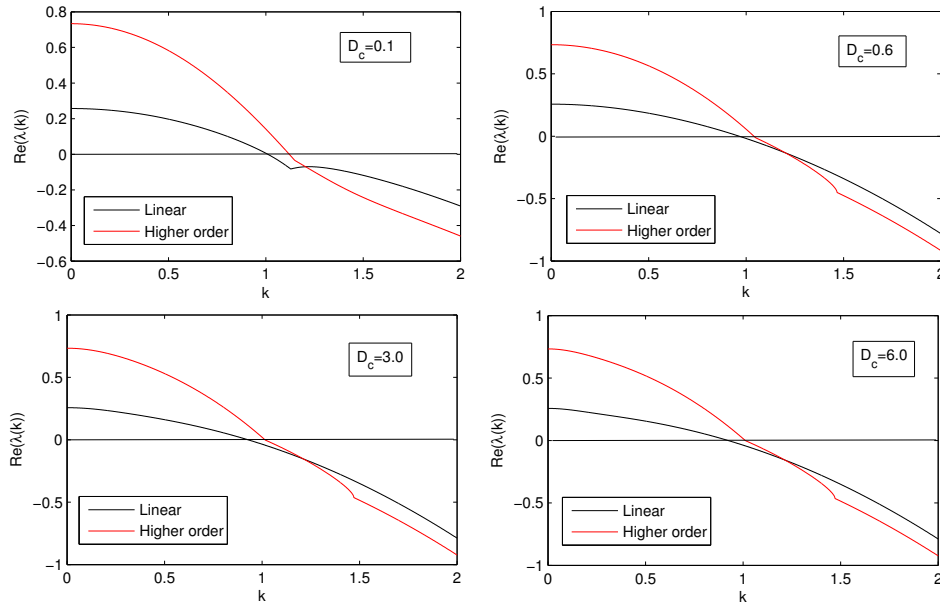


Fig. 8. Plot of maximum value of $\text{Re}(\lambda(k))$ versus k : black line for linear and red line for non-linear systems. The parametric values are given in the text. (Online version in colour.)

real part implies that spatiotemporal perturbation diverge with the advancement of time. The complicated structures of the matrix A prevent us to find the eigenvalues analytically. Therefore, using numerical simulations, we find an interval for k , where at least one eigenvalues of A have positive real part.

Now, we consider system (6)–(8) and choosing some parameter values $a_1 = 0.3, a_2 = 0.2, d_1 = 0.03, d_2 = 0.02, b_1 = 0.5, b_2 = 0.6, m_2 = 0.5, m_1 = 0.4, D_a = 0.3, D_b = 0.2$ for different values of diffusivity coefficient D_c . We now calculate the eigenvalues of the matrix A for the model system (6)–(8) around the steady state $(u^*, v^*, w^*) = (0.0783169, 0.51213, 0.209704)$. We found that one eigenvalue having positive real part for a range of values of k in Fig. 8, we have plotted largest $\text{Re}\{\lambda(k)\}$ defined as linear obtained by solving (21) along with largest $\text{Re}\{\lambda(k)\}$ defined as higher order computed numerically for the characteristic equation (43) for a range of wavelengths. It is clear that linear and higher order are positive for $k \in (0, 0.5)$ over the entire range (see Fig. 8).

6 Conclusion

In this paper, a one prey and two predators system with Beddington–DeAngelis functional response is considered. It is shown that there exists Hopf-bifurcation with respect to mutual interference of predator. In the qualitative analysis, we studied dynamical behavior of the temporal system. It is established that when the rate of mutual interference of predator, i.e., M_1 , crosses its threshold value, i.e., $M_1 = M_{10}$, then prey, first predator and

second predator populations start oscillating around the interior equilibrium. The above result has been shown numerically in Fig. 2 for different values of M_1 . In particular, in Fig. 2(a), we observe that the interior equilibrium is stable, when $M_1 = 0.95$, but when it crosses the threshold value of $M_1 = 0.95$, the above system shows Hopf-bifurcation, as shown in Figs. 2(b)–(d). Furthermore, we have observed that the diffusion instability occurs in the spatial system (see Fig. 3). We have observed the nature of spatial patterns with respect to time (see Figs. 4–6). Also, we observed that if a diffusivity coefficient increases, then the population densities become uniform and spotted pattern observed (see Fig. 7). All these spatial patterns show that the qualitative changes lead to spatial density distribution of the spatial system for each species. Furthermore, we have analyzed the stability of linear and non-linear systems with the help of higher order stability analysis and also observed that the linear and non-linear systems change the behavior of the system from instability to stability (see Fig. 8). Our result shows that the modeling by reaction-diffusion equation is an appropriate tool for investigating fundamental mechanisms of spatiotemporal dynamics in the real world food web system.

References

1. S.B.L. Araujo, M.A.M.de Aguiar, Pattern formation, outbreaks, and synchronization in food chain with two and three species, *Phys. Rev. E* (3), **75**, 061908, 14 pp., 2007.
2. J. Feng, L. Zhu, H. Wang, Stability of ecosystem induced by mutual interference between predator, *Procedia Environmental Science*, **2**:42–48, 2010.
3. A. Hastings, T. Powell, Chaos in a three-species food chain, *Ecology*, **72**:896–903, 1991.
4. R.D. Hilt, Food webs in space: On the interplay of dynamic instability and spatial processes, *Ecol. Res.*, **17**:261–273, 2002.
5. D.O. Maionchi, S.F.dos Reis, M.A.M. de Aguiar, Chaos and pattern formation in a spatial tritrophic food chain, *Ecol. Model.*, **191**:291–303, 2006.
6. F. Jordán, I. Scheuring, I. Molnár, Persistence and flow reliability in simple food webs, *Ecol. Model.*, **161**:117–124, 2003.
7. D.V. Vayenas, S. Pavlou, Chaotic dynamics of a microbial system of coupled food chains, *Ecol. Model.*, **136**:285–295, 2001.
8. J.D. Murray. *Mathematical Biology II: Spatial Models and Biomedical Applications*, 3rd edition, Springer, 2003.
9. N.F. Britton, *Essential Mathematical Biology*, Springer, 2004.
10. R.S. Baghel, J. Dhar, R. Jain, Analysis of a spatiotemporal phytoplankton dynamics: Higher order stability and pattern formation, *World Academy of Science, Engineering and Technology*, **60**:1406–1412, 2011.
11. J. Dhar, R.S. Baghel, A.K. Sharma, Role of instant nutrient replenishment on plankton dynamics with diffusion in a closed system: Pattern formation, *Appl. Math. Comput.*, **218**(17):8628–8936, 2012.

12. H. Malchow, Spatio-temporal pattern formation in coupled models of plankton dynamics and fish school motion, *Nonlinear Anal., Real World Appl.*, **1**:53–67, 2000.
13. A. Medvinsky, S. Petrovskii, I. Tikhonova, H. Malchow, Spatiotemporal complexity of plankton and fish dynamic, *SIAM Rev.*, **44**:311–370, 2002.
14. S. Petrovskii, H. Malchow, A minimal model of pattern formation in a prey predator system, *Math. Comput. Model.*, **29**:49–63, 1999.
15. R.S. Baghel, J. Dhar, R. Jain, Bifurcaion and spatial pattern formation in spreading of disease with incubation period in a phytoplankton dynamics, *Electron. J. Differ. Equ.*, **21**:1–12, 2012.
16. R.S. Baghel, J. Dhar, R. Jain, Chaos and spatial pattern formation in phytoplankton dynamics, *Elixir Applied Mathematics*, **45**:8023–8026, 2012.
17. M. Wang, Stationary patterns for a prey-predator model with prey-dependent and ratio-dependent functional responses and diffusion, *Physica D*, **196**:172–192, 2004.
18. H. Qian, J.D. Murray, A simple method of parameter space determination for diffusion-driven instability with three species, *Appl. Math. Lett.*, **14**:405–411, 2003.
19. W. Wang, Y.Z. Lin, L. Zhang, F. Rao, Y.J. Tan, Complex patterns in a predatorprey model with self and cross-diffusion, *Commun. Nonlinear Sci. Numer. Simul.*, **16**:2006–2015, 2011.
20. Y. Cai, W. Liu, Y. Wang, and W. Wang. Complex dynamics of a diffusive epidemic model with strong allee effect. *Nonlinear Anal., Real World Appl.*, **14**:1907–1920, 2013.
21. W. Wang, H.Y. Cai, Y. Zhu, Z. Guo, Allee-effect-induced instability in a reaction-diffusion predator-prey model, *Abstr. Appl. Anal.*, **2013**, 487810, 10 pp., 2013.
22. W. Wang, Y. Cai, M. Wu, K. Wang, Z. Li, Complex dynamics of a reaction-diffusion epidemic model, *Nonlinear Anal., Real World Appl.*, **13**:2240–2258, 2013.
23. W. Wang, Z. Guo, R.K. Upadhyay, Y. Lin, Pattern formation in a cross-diffusive holling-tanner model, *Discrete Dyn. Nat. Soc.*, **2012**, 828219, 12 pp., 2012.
24. S.P. Bhattacharya, S.S. Riaz, R. Sharma, D.S. Ray, Instability and pattern formation in reaction-diffusion systems: A higher order analysis, *J. Chem. Phys.*, **126**, 064503, 8 pp., 2007.